TURBULENCE MEASUREMENTS AND ANALYSIS IN A MULTISTAGE AXIAL TURBINE

L. Porreca[*], *M. Hollenstein*[**], *A.I. Kalfas*[✦], *R.S. Abhari*[✦✦]

Turbomachinery Laboratory
Swiss Federal Institute of Technology
8092 Zürich, Switzerland
contact: luca.porreca@ethz.ch

ABSTRACT

This paper presents turbulence measurements and detailed flow analysis in an axial turbine stage. Fast response aerodynamic probe were used in order to resolve deterministic fluctuation along the three directions. Assuming incompressible flow, the effective turbulence level and Reynolds stress are retrieved by evaluating the stochastic velocity component out of the measured time-resolved pressure and flow angle fluctuations along the streamwise and radial direction.

A comparison between turbulence intensity and measured total pressure shows that flow structures with higher turbulence level are identified in the region of loss cores at the exit of the second stator passage. Turbulence intensity is evaluated under isotropic and non-isotropic assumption in order to quantify the departure from isotropic conditions. The measurements show that locally the streamwise fluctuating component can be twice bigger then the radial and tangential component. The current analysis shows that multi sensor FRAP probes can be used to provide information about the mean turbulence levels in the flow and the Reynolds stress tensor in addition to the measurements of unsteady total pressure loss.

INTRODUCTION

Turbulence modeling is still a critical issue in fluid dynamics. Despite the recent progress of design tools in modern fluid machinery, the use of appropriate turbulence modeling is instrumental in further development and improvement of internal flows machinery applications. However, In order to validate numerical tools and turbulence models, a large number of experimental investigations have been performed in wind tunnels with simple geometry and under flow conditions involving little disturbances. In those cases, velocity measurements rather then pressure are performed using hot wire anemometry or, more recently, optical methods such as LDA or PIV. With these techniques, unsteadiness on the three spatial directions can be resolved up to a relatively large frequency.

[*] Dipl. Ing. Research Assistant
[**] Dipl. Ing.
[✦] Senior Scientist
[✦✦] Professor, Head of the Department

Flow in a turbomachinery environment is however highly unsteady and three dimensional as a result of periodic chopping of the wake, secondary flow vortices interaction and combustion dynamics. Therefore, particularly in low aspect ratio blading, common isotropic turbulence models validated in simple geometry may not be suitable. Several investigations were performed on turbine blading focusing on the effect of turbulence intensity on the heat transfer [1,2], secondary flows development and transition [3,4 and 5], where the study is based primarily on hot wire anemometry measurements. However, very little has been published in order to quantify the departure from the isotropic conditions in a multistage turbine environment.

The present work is based on the extraction of turbulence parameters along the three spatial directions providing a turbulence analysis and assessing the degree of anisotropy in a multistage turbine stage. Measurements are performed using miniaturized cylindrical Fast Response Aerodynamic Probe developed at the Turbomachinery Laboratory at ETH Zurich [7]. The Reynolds stress tensor and the turbulence level are evaluated taking into account the stochastic values of the measured time-resolved pressure and flow angle fluctuations. Measurements are carried out in a two stages axial turbine facility representative of power generation application.

NOMENCLATURE

c	absolute velocity vector
p	static pressure
p_d	dynamic head
$s,\square,r$	streamwise,circumferential and radial directions
u	streamwise velocity component
v	circumferential velocity component
w	radial velocity component
u',v',w'	stochastic velocity components
t	time
T/T_0	Blade passing period fraction
Tu	Turbulence intensity
5HP	5 Hole Probe
2S-FRAP	2-Sensor FRAP probe
Greek	
α	yaw angle
β	pitch angle
ρ	density
Subscripts/superscripts	
1	probe position 1
iso	isotropic assumption

EXPERIMENTAL METHOD

The research facility

The experimental investigation was performed on the research turbine "LISA" at the Turbomachinery Laboratory of the ETH Zurich. The facility can accommodate a maximum of two stages of an axial turbine. The air-loop is of a closed type and includes a radial compressor, a two-stage water to air heat exchanger and a calibrated venturi nozzle for accurate mass flow measurements. A DC generator absorbs the turbine power and controls the rotational speed of the turbine shaft. The first and the second rotor are mechanically decoupled by a twin spool shaft design. A set of independent torquemeters allows to derive separately the torque of both stages. In order to achieve the same rotational speed, both shafts are coupled again before the DC generator. A sketch of the turbine section is presented in Fig 1. More details can be found in Porreca et al. [8].

The turbine design allows quick and precise assembly and an easy access to the measurement planes. A number of different intrusive (probes) and non-intrusive measurement (Particle Image Velocimetry) techniques are applied. The facility is equipped with a 4-axis numerically controlled positioning system with ultra high precision in every direction. The turbine is normally operated at constant pressure difference across the stages. The turbine entry temperature is controlled to an accuracy of 0.3% and the RPM is kept constant by the DC generator with a range of ±0.02% (± 0.5 RPM). The main operational parameters of the facility are listed in Table 1.

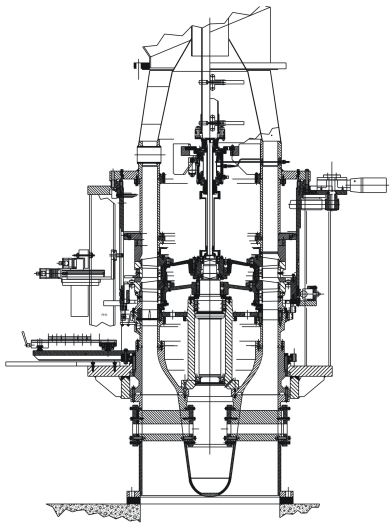

Fig 1: LISA Axial Turbine Facility

The test case under investigation is representative of a partially shrouded axial turbine for power generation. The partial shroud has two vertical fins and a shroud platform with cutbacks at leading and trailing edges. The tip clearance in both rotors is 1% of the blade span.

Rotor speed [RPM]	2625
Overall pressure ratio	1.38
Mass flow [kg/s]	10.65
Blade count (Stator/Rotor)	42 / 42
Aspect ratio	1.8
Outer tip diameter [m]	0.8
Mach number (Stator/Rotor)	0.35 / 0.1

Reynolds number (Rotor)	$2*10^5$

Table 1: Main parameter of "LISA" 2-stages Axial turbine research facility.

Measurement technology

Flow parameters including total and static pressure, flow angles velocity components and Mach number are measured at frequencies up to 40 kHz using 2-Sensor Fast Response Aerodynamic Probe (2S-FRAP). This probe is a modified version of the conventional single sensor probe already used in previous investigations [8,9] and has a second sensor sensitive of pitch angle variation of the flow. FRAP probe technology provides also unsteady temperature measurements at very low frequency (up to 10Hz). The absolute uncertainties of the used probe techniques are listed in Table 2. Temperature measurements obtained with FRAP are affected by an absolute uncertainty of the order of ±0.3 K.

	ϕ	β	Pt	Ps	Ma
2S-FRAP	0.3°	0.3°	100 Pa	150 Pa	0.4%

Table 2: Uncertainty bandwidth of the 2S-FRAP

This paper is focused on the measurements performed downstream the exit of the second stator blades row. the measurement grid comprises 1240 points distributed uniformly in the circumferential direction every 3.5% pitch (31 point in 1.1 pitches) and 40 points in the radial direction, clustered towards the endwalls. Owing to an improved and faster probe traversing system, the data acquisition of one measurement plane currently lasts about 7 hours while the turbine pressure drop is stable within 0.3%. Data from the probe sensors are sampled at 200 kHz corresponding to 109 samples each blade passing period. Phase locking averaging data procedure is done over 80 rotor revolutions.

DATA REDUCTION

Turbulence

The time dependent variables in a turbulent flow are commonly split into mean part, a periodic (deterministic) signal and a stochastic signal using the Reynolds decomposition.

In the probe relative frame of reference shown in fig. 2, the absolute flow velocity can be written as:

$$c(t) = \bar{c} + \tilde{c}(t) + c'(t)$$

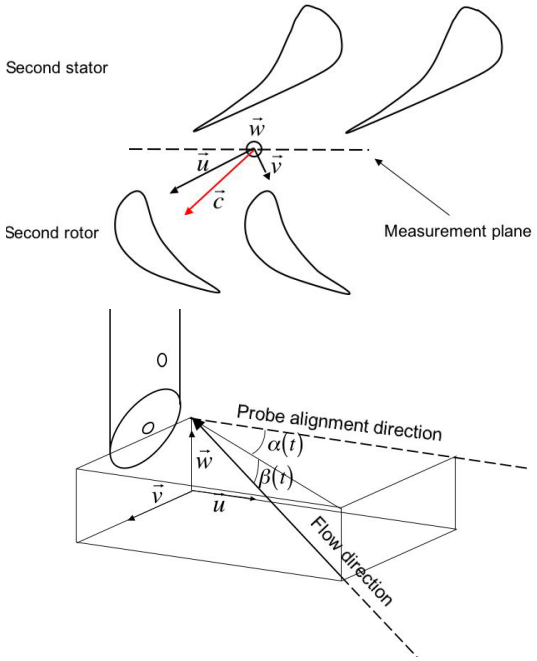

Fig 2: Probe relative coordinate system and definitions

where:

$\bar{c}$ is the arithmetic mean value

$\tilde{c}(t)$ is the deterministic part

$c'(t)$ is the fluctuating part where the mean $\overline{c'(t)} = 0$

The turbulent stresses are used to form the Reynolds stress tensor in terms of velocity fluctuations on the three spatial directions. Taking the mean of the normalised standard deviations of the velocity components yields the conventional definition of the Turbulence level:

$$Tu = \sqrt{\frac{\overline{u'^2} + \overline{v'^2} + \overline{w'^2}}{3\bar{c}^2}}$$

Turbulence measurements with Fast Response Aerodynamic Probes

The measurement probe used has two piezoelectric sensors located on the stem and on the inclined surface at the tip of the probe respectively, as shown in Fig 3. In each measurement point, the probe is turned in three positions. In position 1 the sensors are aligned with the mean direction of the flow evaluated using data form previous measurements. In position 1, unsteady signal from both sensors is acquired simultaneously (P1 and P4). Positions 2 and 3 are necessary in order to measure flow yaw angle by acquiring data only from sensor 1 (P3 and P3).

All four pressure signals are brought together in a set of calibration coefficients representing a dimensionless yaw, pitch, total and static pressure. The data set is phase-lock averaged and the deterministic part of the signal is derived. In this process the stochastic portion of the unsteady signal is not considered.

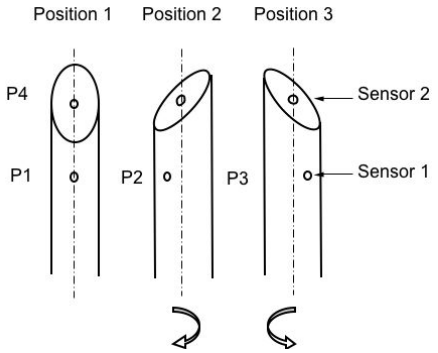

Fig 3: Measurement procedure of the 2S-FRAP

The Bernoulli equation can be applied in order to obtain the stochastic part. Assuming that the flow is considered as incompressible, that in such a low speed turbine facility is reasonable (Mach number between 0.1 and 0.3). Because the probe is positioned in the direction of the flow, then for the first measurement location:

$$p_1 = p_s + \frac{1}{2}\rho u^2$$

therefore:

$$u = \sqrt{\frac{2(p_1 - p_s)}{\rho}} = \sqrt{\frac{2p_d}{\rho}}$$

where p_d is the dynamic head. If the velocity is decomposed into deterministic and stochastic part then:

$$u'(t) = u(t) - \bar{u} = \sqrt{\frac{2p_d}{\rho}} - \sqrt{\frac{2\overline{p_d}}{\rho}}$$

$$u'^2 = \frac{2}{\rho}\left(p_d + \overline{p_d} - 2\sqrt{p_d\,\overline{p_d}}\right)$$

Averaging the measured points in the pitch, data show that static pressure fluctuations can be considered small with respect to the dynamic head ($p_s'/\overline{p}_d < 8\%$). The dynamic head can be separated into steady and fluctuating part. Expanding the term $\sqrt{p_d}$ into a Taylor series, the previous expression can be written as: (Ruck [10])

$$\overline{u'^2} = \frac{1}{2\rho}\frac{\overline{p_1'^2}}{\overline{p_d}}$$

As mentioned before, the probe sensors are aligned with the flow direction. Fig 4 shows the pitchwise averaged mean velocity *v* and *w* with respect to the absolute velocity *c*.

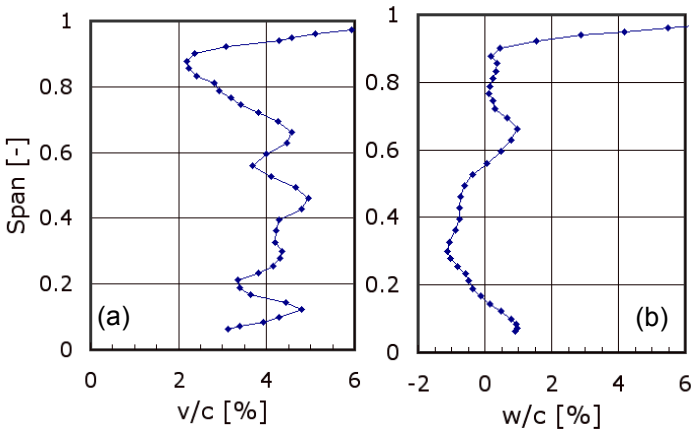

Fig. 4: a) Ratio between mean velocity v and w with respect to the absolute velocity c.

Therefore it can be written:

$$\bar{v} << \bar{c} \quad , \quad \bar{w} << \bar{c}$$

then

$$\bar{u} \cong \bar{c}$$

therefore:

$$\frac{\overline{u'^2}}{\bar{c}^2} = \frac{1}{4}\frac{\overline{p_1'^2}}{\overline{p_d}^2}$$

The yaw angle using the probe as reference can be written as:

$$\tan(\alpha(t)) = \tan\left(\bar{\alpha} + \alpha'(t)\right) = \frac{v(t)}{u(t)} = \frac{\bar{v} + v'(t)}{\bar{u} + u'(t)}$$

it follows that:

$$\bar{v} \cong 0, \bar{w} \cong 0 \text{ and } \bar{\alpha} \cong 0, \bar{\beta} \cong 0$$

therefore the above equation can be simplified as:

$$\tan(\alpha(t)) = \tan(\alpha'(t)) \cong \alpha'(t) = \frac{v'(t)}{\bar{c}}$$

An equivalent derivation can be done over the pitch angle, thus the circumferential and radial normal stress components are:

$$\frac{\overline{v'^2}}{\bar{c}^2} = \overline{\alpha'^2} \quad \text{and} \quad \frac{\overline{w'^2}}{\bar{c}^2} = \overline{\beta'^2}$$

The shear stress component of the Reynolds tensor can be expressed as the product of two velocities fluctuation respectively. Following the method developed above yields:

$$\frac{\overline{u'v'}}{\overline{c}^2} = \frac{\overline{\alpha' p_1'}}{2p_d}$$
$$\frac{\overline{u'w'}}{\overline{c}^2} = \frac{\overline{\beta' p_1'}}{2p_d}$$
$$\frac{\overline{w'v'}}{\overline{c}^2} = \overline{\alpha'\beta'}$$

Attention needs to be paid to the evaluation of the term $\overline{v'^2}$. As mentioned before, the 2S-FRAP probe is turned in position 2 and 3 to measure flow yaw angle. This procedure implies that yaw angle fluctuation is evaluated by 3 non-simultaneous measurements. Therefore in order to derive the term $\overline{v'^2}$, a continuity equation in cylindrical coordinates can be applied under the assumption of incompressible flow. Therefore:

$$\frac{\partial u'}{\partial x} + \frac{1}{r}\frac{\partial v'}{\partial \theta} + \frac{1}{r}\frac{\partial rw'}{\partial r} = 0$$

Assuming that:

$$\frac{\partial}{\partial x} << \frac{\partial}{\partial \theta}$$

then:

$$v' = -\int \frac{\partial rw'}{\partial r} d\theta + const$$

it can be assumed that at midspan, in the free stream region, the root square mean of the fluctuating velocity in radial and circumferential direction have the same magnitude. From this assumption the constant in the previous equation can be evaluated and thus the term $\overline{v'^2}$ in all the measurement plane.

RESULTS AND DISCUSSION

This study focuses on the flow field measured downstream the second stator row. Results are presented as area plots and pitch-wise mass averaged profile. Fig. 5 shows the time-averaged total pressure coefficient and yaw angle profile on the blade span. At the hub, the passage vortex is established with typical overturnig - underturning behavior. This is also responsible for the total pressure reduction at around 10% span. Further up in the radial direction, a marked underturning - overturning behavior is observed at 70% of the span. This feature is caused by the tip passage vortex. The area plot (Fig 6) is representing the measured total pressure coefficient together with the secondary flows.

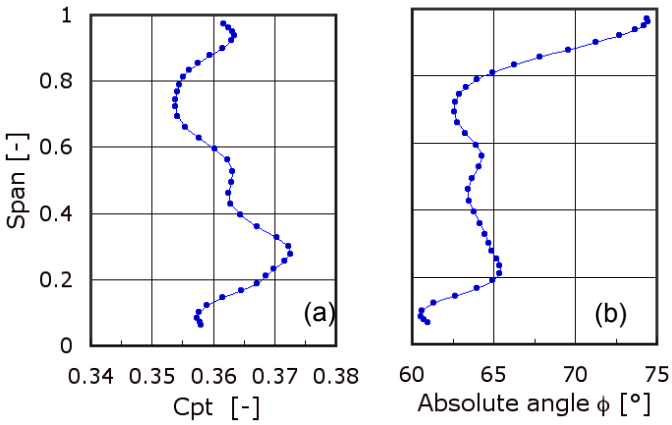

Fig. 5: Mass averaged a) total pressure coefficient and b) yaw angle at the exit of the second stator

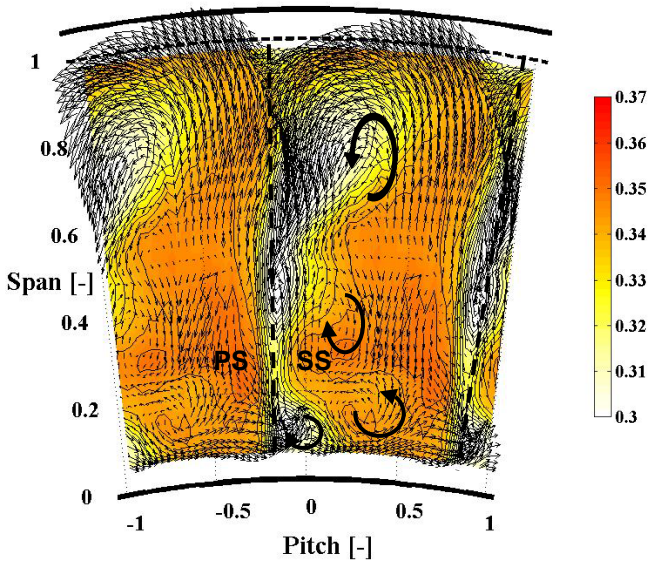

Fig. 6: Measured total pressure coefficient and secondary flows at exit of the second stator

The wake is identified in both cases at approximately -20% blade pitch and shown with a dotted line. The hub passage vortex is identified at the hub and it contributes to the total pressure reduction in this region. Further upstream two vortex structures are also identified, these features are thought to originate at the first rotor and convected through the downstream stationary blade row. Finally, at the tip a large loss core is identified due to the tip passage vortex.

Turbulence analysis

The turbulence level downstream of the second stator was calculated using the isotropic assumption, therefore:

$$\overline{u'^2} \cong \overline{v'^2} \cong \overline{w'^2}$$

$$Tu_{iso} = \frac{1}{2}\frac{\sqrt{\overline{p_1'^2}}}{\bar{c}^2}$$

without the use of this assumption, according with the previous derivation, the turbulence intensity can be expressed as:

$$Tu = \sqrt{\frac{1}{3}\left(\frac{1}{4}\frac{\overline{p_1'}}{\bar{c}^2} + \frac{\overline{v'^2}}{\bar{c}^2} + \overline{\beta'^2}\right)}$$

In order to quantify the departures from isotropy, the degree of anisotropy is evaluated by comparing fluctuating components in the three directions. Therefore:

$$DA = \frac{\overline{2u'^2}}{\overline{v'^2} + \overline{w'^2}}$$

Figures 7a and 7b show the turbulence intensity levels calculated with and without the isotropy assumption. In both plots, strong similarities are observed with respect to the total pressure distribution shown in fig. 6. In the wake and in the secondary flow regions the turbulence intensity is higher with a level up to 12%. Similar levels of turbulence intensity have been observed in fundamental studies of turbulent flows with high shear and coherent structures [11].

Figure 7c shows the degree of anisotropy as defined above. Higher values of the degree of anisotropy can be observed at the endwall region and close to the wake. In the pressure side region, where the flow is weakly affected by secondary flows structures surprisingly the contribution of the term $\overline{w'^2}$ and $\overline{v'^2}$ are higher than $\overline{u'^2}$, the Degree of Anisotropy decreases up to 0.5. Moving circumferentially close to the wake the fluctuating terms are rising. However, the relative increase of the streamwise and circumferential component is twice as big compared to the radial (DA equal to 1).

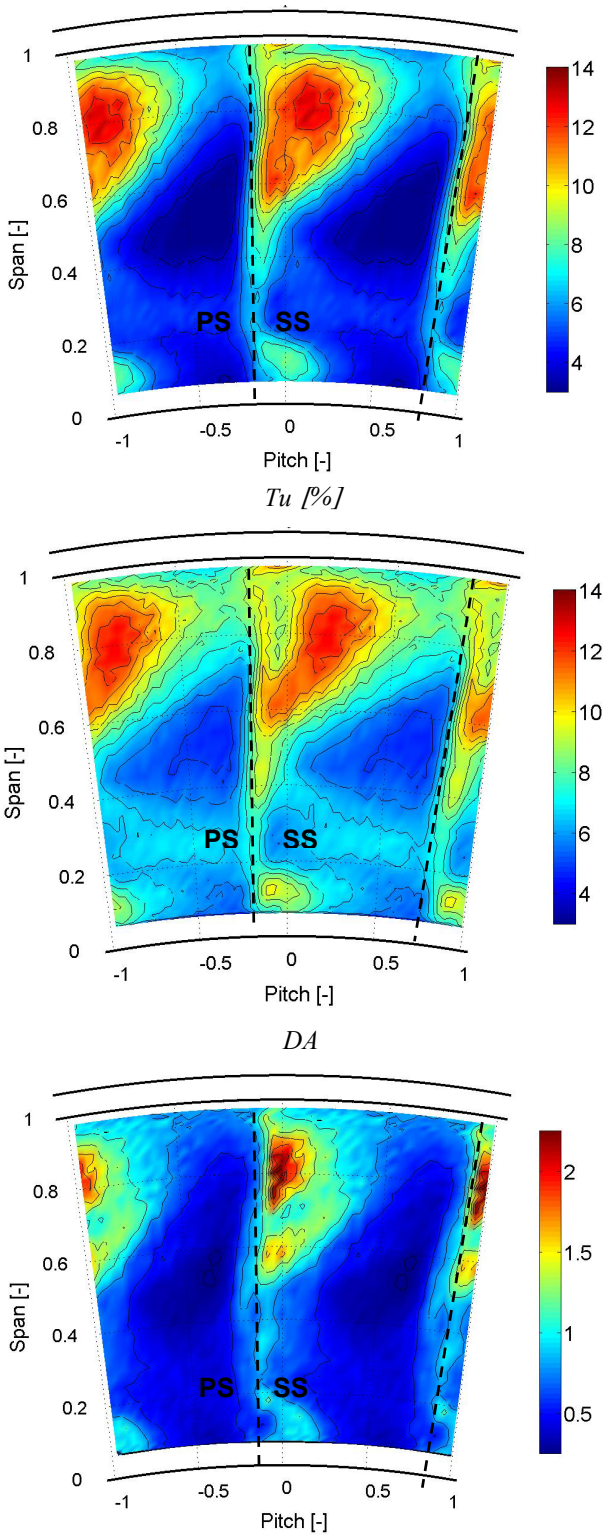

Fig. 7: Turbulence intensities evaluated a) with and b) without the isotropic assumption c) DA

In Fig 7b at the tip region, the turbulence level without the isotropy assumption has a relatively higher mean value (up to 10% of intensity) that is not present in Fig 7a. This behavior can be explained taking into account that the flow in that region contains a large amount of turbulent fluid coming through the first rotor tip. In the same region a high entropy production is in fact detected that not present at the lower part of the blade span.

Comparison of the instantaneous turbulence level with the total pressure coefficient shows that regions with high pressure drop as in the wake and in the secondary flows correspond to high turbulence intensity level areas. The maximum instantaneous turbulence intensity reaches the value of 16% of the free stream velocity.

Figure 8 shows a close up of the turbulence intensities in this region with the calculated secondary flows superimposed. Position of the stator trailing edge is indicated by a dashed line while a continuous line shows the rotor relative leading edge location. At position T/T_0=0, a vortex structure at the center of the passage is identified. This vortex appears very strong in this position and is thought to be the suction side leg of the passage vortex that originates in front of the rotor leading edge. At this position, stator trailing edge and rotor are almost aligned, therefore the area seen by the fluid is the largest. This gives space to the boundary layer to turn round the rotor leading edge and generate the classical horse-shoe vortex leg rotating in the counter-clock wise direction on the blade pressure side. While the rotor blade moves towards the stator trailing edge the strength of this vortex structures appears to be decreased (T/T_0 equal to 0.25 and 0.5). This behavior can be explained taking into account that at these positions there is a strong interaction with the hub passage vortex of the second stator that rotates in the opposite direction. Due to the interaction of these contra-rotating vortex structures, the turbulence level in this area increases up to 18%. When the rotor moves forward the trailing edge position, the horse-shoe vortex is established again. (T/T_0 = 0.75).

At each rotor position, the turbulence intensity levels, the streamwise $\sqrt{\overline{u'^2}}$ and radial $\sqrt{\overline{w'^2}}$ fluctuating components are mass averaged in order to obtain one value at each rotor-stator position. The resulting plots are presented in Fig. 9. All three parameters are plotted at the same scale, same value interval (0.5 % of the local mean velocity) but different absolute level. The mean level of the radial fluctuating component $\sqrt{\overline{w'^2}}$ is higher than the streamwise term $\sqrt{\overline{u'^2}}$ with a difference up to 45%. Significant differences are found in the amplitude of variation of the fluctuating terms. The radial component is varying as function of the blade period between 9% and 9.5% however the streamwise variation is limited between 6.25% and 6.45%. Moreover the radial term $\sqrt{\overline{w'^2}}$ shows a clear periodicity as the blade passing period with higher peaks at T/T_0 equal 0 and smaller kinks at T/T_0 equal 0.66. The same peaks are not observed in the streamwise fluctuation.

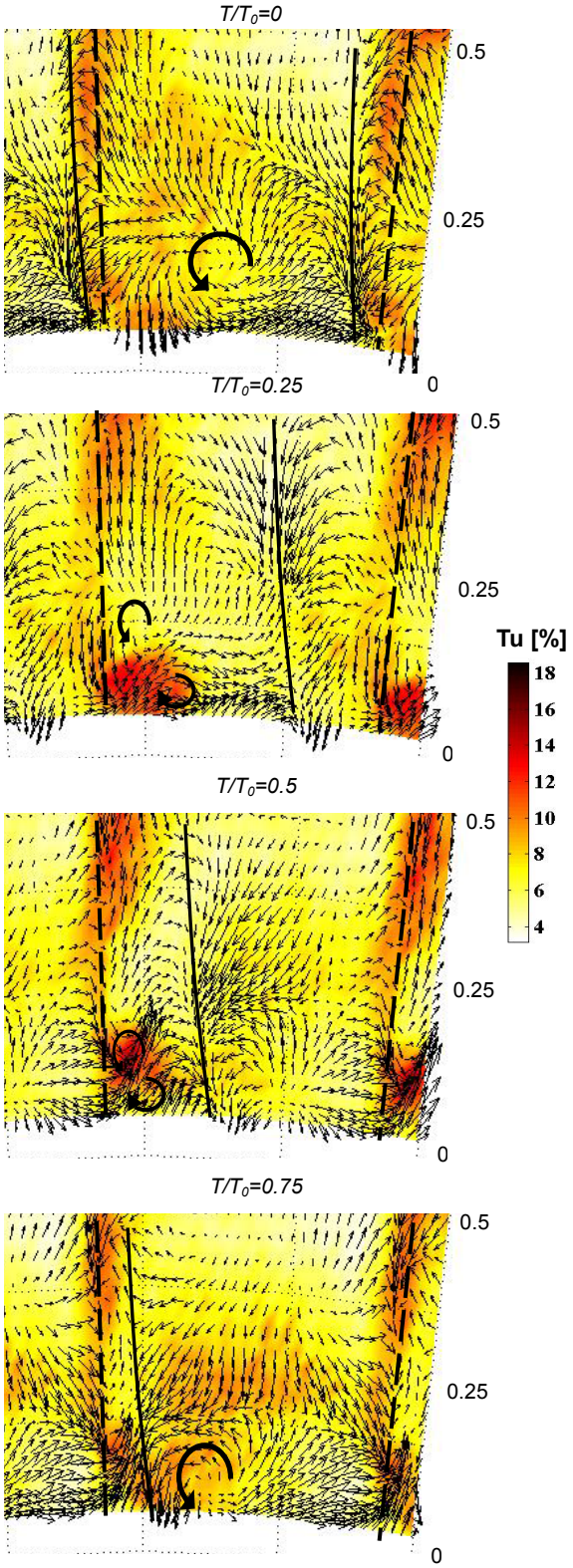

Fig. 8: Measured turbulence intensities and secondary flows in one blade passing period

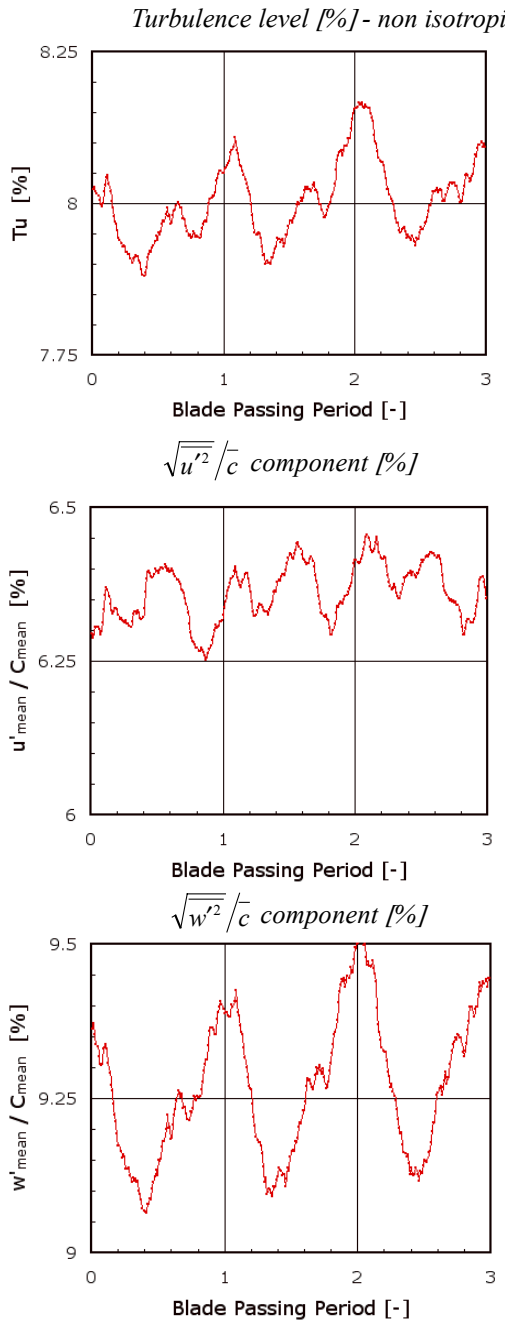

Fig. 9: Measured mass averaged value of a) Tu intensity b) streamwise and c) radial fluctuating component in 3 blade passing periods

Two peaks of similar amplitude are observed with a frequency twice the blade passing frequency. The interaction between the vortex structures and shed vorticity in the wake contributes to this behavior.

CONCLUSION

In this paper, a novel approach on the measurement of turbulence parameters in turbomachinery is presented. Using the unsteady pressure signal from multisensor FRAP probe the turbulence intensity and Reynolds stress component are derived at the exit of the second stator blade in a 2-stages axial turbine.

The time average turbulence level reaches level up to 14% in the core of the secondary flows and in the wake. A contribution to assess the degree of anisotropy in turbomachinery flows is made. Turbulence intensity levels are evaluated with and without isotropy assumption. The level of the mean turbulent kinetic energy in radial $\overline{w'^2}$ and circumferential direction $\overline{v'^2}$ appears in most of the region higher then the streamwise term $\overline{u'^2}$. However, close to high shear stress area the relative increase of the streamwise component is twice higher then the other components. By time averaging the kinetic energy terms on the entire flow area it is shown that the radial component has a higher level up to 45% respect to the streamwise fluctuation. This underlines that in turbomachinery flows isotropic turbulence models for computations and predictions are not always appropriate.

In the hub region the interaction of the stator passage vortex and the horse-shoe vortex of the second rotor raises locally the turbulence intensity level up to 16%. This behavior is occurring periodically with the blade passing frequency.

REFERENCES

[1] R. W. Radomsky, K. A. Thole "*High Free-Steam Turbulence Effects on Endwall Heat Transfer for a Gas Turbine Stator Vane"* ASME Journal of Turbomachinery J. Turbomach. 122,

[2] Gregory-Smith, D. G., and Cleak, J. G. E., 1992, "*Secondary Flow Measurements in a Turbine Cascade With High Inlet Turbulence*," ASME J. Turbomach., 110, pp. 1–8.

[3] Volino, R. J., and Hultgren, L. S., 2001, "*Measurements in Separated and Transitional Boundary Layers Under Low-Pressure Turbine Airfoil Conditions,*" ASME J. Turbomach., **123**, pp. 189–197.

[4] Chaluvadi, V.S.P., Kalfas A.I., Banieghbal, M.R., Hodson H.P., Denton, J.D. (2001) *"Blade Row Interaction in a High Pressure Turbine",* AIAA Journal of Propulsion and Power, 174, pp 892-901.

[5] Binder A., Schroeder Th., Hourmouziadis J., *"Turbulence Measurements in a Multistage Low-Pressure Turbine".* ASME Journal of Turbomachinery, Vol 111.

[6] Walraevens, R.E., Gallus, H.E., Jung, A.R., Mayer J. F., Stetter H., *"Experimental and Computational Study of the Unsteady Flow in a 1.5 Stage Axial Turbine with Emphasis on the Secondary Flow in the Second Stator"* ASME 98-GT-254

[7] Kupferschmied P., Köppel O., Gizzi W.P., Gyarmathy G., *"Time resolved flow measurements with fast aerodynamic probes in turbomachinery"*, Meas. Sci. Technol. Vol 11, pp 1036,1054.

[8] Porreca, L., Behr, T., J. Schlienger, , Kalfas, A. I., Abhari, R. S., Ehrhard J., Janke E, "*Fluid Dynamic and Performances of Fully and Partially Shrouded Axial Turbine*", ASME Paper No. GT2004-53869. Accepted for publication in Journal of Turbomachinery

[9] Schlienger J., Kalfas A. I., Abhari R. S., "*Vortex-Wake-Blade Interaction in a Shrouded Axial Turbine*". ASME GT-2004-53915. Accepted for publication in Journal of Turbomachinery

[10] G. Ruck, *"Ein Verfahren zur instationären Geschwindigkeits- und Turbulenzmessung mit einer pneumatisch messenden Keilsonde"* 1989, Diss. Univ. Stuttgart.

[11] Kalfas, A.I., Elder, R.L. *"Effects of free stream turbulence on intermittent boundary layer flows"* ASME Turbo Expo 1995. Houston, Texas, June 5-8.